

RSC Advances



This is an *Accepted Manuscript*, which has been through the Royal Society of Chemistry peer review process and has been accepted for publication.

Accepted Manuscripts are published online shortly after acceptance, before technical editing, formatting and proof reading. Using this free service, authors can make their results available to the community, in citable form, before we publish the edited article. This *Accepted Manuscript* will be replaced by the edited, formatted and paginated article as soon as this is available.

You can find more information about *Accepted Manuscripts* in the [Information for Authors](#).

Please note that technical editing may introduce minor changes to the text and/or graphics, which may alter content. The journal's standard [Terms & Conditions](#) and the [Ethical guidelines](#) still apply. In no event shall the Royal Society of Chemistry be held responsible for any errors or omissions in this *Accepted Manuscript* or any consequences arising from the use of any information it contains.

Reverse poly(butylene oxide)-poly(ethylene oxide)-poly(butylene oxide) block copolymers with lengthy hydrophilic blocks as efficient single and dual drug-loaded nanocarriers with synergistic toxic effects on cancer cells

E. Villar-Alvarez^{a‡}, E. Figueroa-Ochoa^{b‡}, S. Barbosa^{a}, J. F. A. Soltero^b, P. Taboada^a and V. Mosquera^a*

^a*Grupo de Física de Coloides y Polímeros, Departamento de Física de la Materia Condensada; Universidad de Santiago de Compostela, 15782-Santiago de Compostela, Spain.*

^b*Laboratorio de Reología, Departamento de Ingeniería Química, CUECI, Universidad de Guadalajara, Blv. M. García Barragán 44430 Guadalajara, Jalisco, México*

* Author to whom correspondence should be addressed: silvia.barbosa@usc.es

‡ These authors contribute equally to this work.

Abstract

Combination therapy appears as a very interesting alternative to solve some of the problems associated with single-drug therapies such as resistances and improve patient's survival. Nevertheless, it also possess a series of potential drawbacks, mainly associated with the complicated administration of several antineoplastic drugs which use different excipients owing to compatibility and stability issues. Hence, the combination of two or more drugs in one polymeric micelle with sufficient loading capacity could solve this issue as well as providing a suitable control of release rate and protection for cargos. In this paper, four different reverse poly(butylene oxide)–poly(ethylene oxide)–poly(butylene oxide) block copolymers, $BO_nEO_mBO_n$, with BO blocks ranging from 8 to 21 units and EO ones from 90 to 411 were tested as potential single and dual nanocarrier of the antineoplastic drugs docetaxel and doxorubicin currently used in combination for the treatment of advanced/metastatic breast cancer. Polymeric micelles formed by these copolymer were shown to solubilise important amounts of these drugs, either alone or combined, in a single micelle with a good stability in serum mimicking conditions. These polymeric nanocarriers were able to release drugs in a sustained manner, being the release rate slower as the copolymer chain hydrophobicity increased. Drugs loaded in the polymeric micelles accumulated more slowly inside the cells than free DOXO due to its sustained release. Copolymers were found to be biocompatible in most of the concentration range tested. The *in vitro* cell cytotoxicity was found to be larger for dual DCX/DOXO-loaded micelles than for single-loaded ones and free administered drugs in both cervical HeLa and breast MDA-MB-231 cancer cell lines tested by exerting a synergistic effect. Therefore, poly(butylene oxide)–poly(ethylene oxide) block copolymers offer important features as efficient nanocarriers for dual combination therapy, which joined to the ability of

some of the present copolymer varieties to inhibit efflux pump mechanisms can allow the development of interesting nanoformulation without standing therapeutic efficacies in cancer treatment.

KEYWORDS: Reverse copolymers, combination therapy, drug delivery, polymeric nanocarrier, synergistic toxicity.

1. Introduction

The properties of amphiphilic copolymers combining hydrophilic poly(ethylene oxide) units with different types of hydrophobic blocks have been found to show suitable characteristics to fulfill the requirements for a relatively efficient therapeutic action of poorly-aqueous soluble drugs by enhancing their solubilization, allowing their sustained release, improving their pharmacokinetics and facilitating their access to the site of action while providing “stealthness” to evade scavenging by the mononuclear phagocyte system¹⁻³. These beneficial properties can originate from the spontaneously self-assembly of copolymer chains into nanoscopic core-shell micellar structures in solution⁴. The micellar cores offer an excellent platform for the solubilization of the poorly water-soluble therapeutic agents^{5,6}; this is particularly interesting for hydrophobic anticancer agents in preclinical development, e.g. 17-allylamino-17-demethoxygeldanamycin, 17-AAG, and in clinical practice, e.g. paclitaxel, docetaxel, doxorubicin and etoposide amongst others, which require safe vehicles for solubilization and intravenous infusion provided that current vehicles for intravenous drug infusion are often toxic, e.g. Chremofor EL. Moreover, the polymeric micellar carrier also offers protection for cargos provided by the hydrophilic shell that minimizes the nonspecific uptake through the reticuloendothelial system (RES), thereby, enhancing drug circulation times and passive accumulation in solid tumors⁷.

Single drug therapy of cancer is rarely successful due to inherent and developing drug resistance to tumors, the heterogeneity of cancer cells, and the existence of leakages and/or burst release phases from the nanocarriers which do not allow to reach sustained effective therapeutic concentration for the payloads. Different attempts have been made to solve these issues as, for example, the

development of core-shell nanostructures (polymeric fibers and micelles) which enable a biphasic sustained release of the cargo molecules to ensure optimal therapeutic concentrations.^{8,9} Other alternative is the combined use of different drugs, the so-called combination chemotherapy, which has become a standard regimen to treat cancer patients¹⁰. Such therapy regimens commonly involve the sequential administration of multiple drugs that can act along different synergistic pathways and kill cancer cells better while retarding occurrence of resistant cell lines within acceptable toxicity¹¹. Despite the advantages of combination chemotherapy, one of the main challenges associated with its clinical application is the complicated administration of several antineoplastic drugs which use different excipients owing to compatibility and stability issues. For example, the solubilization of one drug inside a polymeric micelle embedded into the core of a electrospun fiber which, at the same time, serves as an additional depot for an additional drug has been shown to be an effective way to achieve a codelivery and multistep sustained release of several drugs.¹² Other option can be simply combining drugs into one single polymeric micelle with sufficient loading capacity, which could simplify fabrication processes and treatments, making the latter less hazardous to patients. A mediocre loading might be an impediment for even single drug micelle formulations provided that administration would require prohibitively high doses of the polymer proper, which could result in vehicle-derived toxicity as observed, for example, in the case of Taxol and Taxotere, clinical formulations of paclitaxel and docetaxel which contains Cremophor EL and Polysorbate 80 as excipients, respectively, and can induce hypersensitivity reactions and toxicities during intravenous infusions¹³.

Polymeric micelles which combine poly(oxyethylene) and poly(oxypropylene) blocks [EO = oxyethylene, OCH_2CH_2 and PO = oxypropylene, $\text{OCH}_2\text{CH}(\text{CH}_3)$] in a

triblock structure, either direct, $EO_mPO_nEO_m$, or reverse, $PO_nEO_mPO_n$ (where the subscripts m and n denote number-average block lengths) have been the most extensively studied for drug antineoplastic administration due to their commercial availability in a very broad range of compositions, a sustained release pattern, a good biocompatibility of most varieties, and approval of some varieties by regulatory agencies to be used in pharmaceutical formulations.¹⁴ Nevertheless, $EO_mPO_nEO_m$, or $PO_nEO_mPO_n$ copolymers possess several drawbacks as, for example, very limited solubilization capacity, low stability upon dilution in the bloodstream, and changes in the micellization behavior from batch to batch due to polydispersity as a consequence of the transfer reaction from hydrogen abstraction during the polymerization of PO blocks¹⁵. Hence, during last years different block copolymer counterparts with similar architecture but with the PO segment replaced by a more hydrophobic one have been proposed with the aim of improving drug solubilization capacities and release profiles.¹⁶⁻²¹ Special attention has been paid to copolymers with 1,2-butylene oxide (BO) as the hydrophobic monomer due to structural similarity to PO and provided that transfer is not a problem in the laboratory polymerization of BO.²² This monomer (as PO does) adds to the growing chain to give a secondary oxyanion, and the slow initiation of EO chains at the secondary termination might lead to a broadened EO-block length distribution.²³ To avoid such deleterious effects, BO blocks can be polymerized last forming EO_mBO_m diblock and $BO_nEO_mBO_n$ triblock copolymers. In addition, the larger relative hydrophobicity of BO blocks compared to PO (six-fold as estimated from the ratio of the logarithms of the molar critical micellar concentrations, cmcs)¹⁶ allows the formation of polymeric micelles, transient micelle clusters and polymer networks by bridging of extended chains between micelles^{24,25} at much lower concentrations than $PO_nEO_mPO_n$ do. Provided that these copolymers have

been proved to be biocompatible in some preliminary experiments²⁶ their use as anticancer nanocarriers would allow the solubilization of higher concentrations of poorly aqueous soluble drugs at much lower copolymer concentrations²⁷ in the form of injectable solutions, oral suspensions and/or (sub)dermal gelling depots^{27,28} while exerting a complementary role as “cell response modifiers”, for example, by inhibiting the P-glycoprotein efflux pump in multidrug-resistant (MDR) tumoral cells. We have recently shown that $BO_nEO_mBO_n$ copolymers can efficiently incorporate doxorubicin (DOXO) exerting an enhanced and sustained therapeutic against multidrug resistant ovarian cancer cells.²⁷

This paper addresses two questions: first, whether different water-insoluble antineoplastic drugs can be incorporated in such polymeric micelles with suitable loading capacities, and second, whether multiple drugs can be simultaneously incorporated inside micellar cores to form pharmacologically synergistic chemotherapeutic combinations of high potency to kill cancer cells. To do that, four different reverse $BO_nEO_mBO_n$ triblock copolymers ($BO_8EO_{90}BO_8$, $BO_{14}EO_{378}BO_{14}$, $BO_{20}EO_{411}BO_{20}$ and $BO_{21}EO_{385}BO_{21}$) were tested as effective nanocarriers for single/dual drug delivery of hydrophobic antineoplastic compounds such as docetaxel (DCX) and DOXO used nowadays in combination chemotherapy for the treatment of advanced/metastatic breast cancer through parenteral administration. The results suggest $BO_nEO_mBO_n$ micelles can provide an attractive, biocompatible platform for co-solubilization and delivery of multiple hydrophobic molecules with minimal vehicle-associated side effects and avoiding the limitations of organic solvents and/or surfactants in current chemotherapeutic formulations to enhance the solubilization of this class of drugs in terms of side effects.

2. Materials and methods

2.1 Materials

Four $\text{BO}_n\text{EO}_m\text{BO}_n$ copolymers with narrow chain length distributions ($\text{BO}_8\text{EO}_{90}\text{BO}_8$, $\text{BO}_{14}\text{EO}_{378}\text{BO}_{14}$, $\text{BO}_{20}\text{EO}_{411}\text{BO}_{20}$ and $\text{BO}_{21}\text{EO}_{385}\text{BO}_{21}$) were prepared and characterized as previously described.²⁹ The critical micelle concentrations (cmc) in aqueous solution were estimated from pyrene fluorescence measurements, as previously reported.³⁰ Table 1 summarizes the molecular characteristics of the copolymers.

Table 1. Molecular weight and critical micelle concentration (cmc) of the copolymers.

Copolymers	M_n^a (g/mol)	M_w / M_n^b	M_w (g/mol)	CMC ^c (mg/mL)	N	r_h (nm)
$\text{BO}_8\text{EO}_{90}\text{BO}_8$	5100	1.07	5460	0.33	38 ^d	13.0 ^d
$\text{BO}_{14}\text{EO}_{378}\text{BO}_{14}$	18600	1.12	20832	0.058	18 ^e	18.5 ^e
$\text{BO}_{20}\text{EO}_{411}\text{BO}_{20}$	21000	1.08	22680	0.012	17 ^d	18.9 ^d
$\text{BO}_{21}\text{EO}_{385}\text{BO}_{21}$	20000	1.10	22000	0.025	9 ^e	20.4 ^e

^a Estimated by NMR; ^b Estimated by GPC; M_w calculated from M_n and M_w/M_n . Estimated uncertainty: M_n to ± 3 %; M_w/M_n to ± 0.01 . ^c Values from ref. 37; ^d values from ref. 61; ^e values from ref. 62.

Docetaxel and doxorubicin hydrochloride (DOXO·HCl) were acquired from Sigma-Aldrich. DOXO base was obtained by means of the aqueous precipitation of DOXO·HCl aqueous solution (1 mg/mL) by adding triethylamine and methylene chloride. The system was kept under vigorous stirring for 1 h., and then the organic phase was evaporated in order to recover DOXO base.³¹ Herein after, DOXO refers to

DOXO base. Water was double distilled and degassed before use. All other reagents were analytical grade.

2.2. Drug solubilisation

Solubilization of DCX and DOXO (intrinsic solubility in water ca. 4.9 and 0.5 mg dm⁻³, respectively)³² in micellar copolymer solutions was tested in triplicate following the procedure of Elsabahy *et al.* with minor modifications.³³ Briefly, the desired amount of drug(s)(typically 40 µg in total) dissolved in dichloromethane (100 µM) was added to the weighted solid copolymer (typically 2 mg). The organic solution was stirred and the solvent evaporated until dryness. Then, distilled water was added dropwise to the dried sample and left under stirring overnight. Solution were centrifuged at 3000 rpm for 30 min, and the supernatants filtered (Millipore Millex filters, 0.45 µm pore size) to remove the non-solubilised drug. The filtered solutions were diluted (1/1000) with methanol to disrupt the self-assembled structures. The amount of solubilised DCX and DOXO were determined by UV-Vis(Cary 50 UV-Vis spectrophotometer, Agilent, Germany) at 227 and 480 nm, respectively, using solutions of each copolymer at the same dilution conditions as blanks, by fluorescence spectroscopy by excitation at 480 nm (only for DOXO), and/or by reverse phase high performance liquid chromatography (HPLC). For HPLC, an Agilent Technologies 1200 series HPLC system equipped with a Nucleosil C18 5 µm column (250 mm × 4.6 mm) was used. Samples were diluted using mobile phase (specified below) and injected (20 µL) into the HPLC system. For both single DCX, DOXO and dual DCX/DOXO solutions a mixture of acetonitrile/water (55/45 v/v) was used as mobile phase. The flow rate was 1.0 mL/min, and column temperature was set to 30 °C. Detection wavelengths were 227 and 480 nm and

retention times were 8.1 and 7.0 min for DCX and DOXO, respectively.

Drug loading, D.L., entrapment efficiency, E.E., and the solubilisation capacity per gram of copolymer in solution, S_{CP} (namely, the amount of drug dissolved at 37 °C in 100 mL of copolymer solution in excess of that dissolved in an equivalent volume of water) were calculated as follows:

$$D.L.\% = \frac{\text{weight of the drug in micellar solution}}{\text{weight of polymer + drug}} \times 100\% \quad (1)$$

$$E.E.\% = \frac{\text{weight of the drug in micellar solution}}{\text{weight of feeding drug}} \times 100\% \quad (2)$$

$$S_{CP} = \frac{\text{weight of the drug in micellar solution (mg)}}{\text{weight of polymer (g)}} \quad (3)$$

2.3. Micellar sizes and physical stability of the drug-loaded micelles upon dilution

Sizes of unloaded and drug-loaded polymeric micelles were determined by dynamic light scattering (DLS) using an ALV-5000F (ALV-GmbH, Germany) instrument with vertically polarized incident light ($\lambda = 488$ nm) supplied by a diode-pumped Nd:YAG solid-state laser (Coherent Inc., CA, USA) operated at 2 W, and combined with an ALV SP-86 digital correlator (sampling time of 25 ns to 100 ms; scattering angle $\theta = 90^\circ$). Experiment duration was in the range 5-10 min, and each measurement was repeated at least twice. The correlation functions from DLS runs were analyzed by the CONTIN method to obtain the intensity distributions of decay rates (I), the apparent diffusion coefficients, and then the apparent hydrodynamic radius ($r_{h,app}$) applying the Stokes-Einstein equation.¹⁶ Sizes and morphology of drug-loaded polymeric micelles were also measured by transmission electron microscopy (TEM). Micellar drug-loaded polymer solutions were applied over carbon-coated copper grids, blotted, washed, negatively stained with 2 wt. % phosphotungstic acid,

air-dried and, then, examined with a Phillips CM-12 transmission electron microscope operating at an accelerating voltage of 120 kV.

The physical stability of the drug-loaded micelles was assessed by dilution of the samples (1/50) in PBS buffer (pH7.4) supplemented with 10% fetal bovine serum (FBS) at 37 °C under moderate stirring, and the drug concentration monitored over time by UV spectrophotometry, as described above. The experiments were performed in triplicate. Simultaneously, aliquots were taken, filtered (Triton free Millipore Millex, 0.22 µm porosity) into scattering cells and allowed to equilibrate at 37°C for 30 min before recording changes in the size of drug-loaded micelles by DLS as described above.

2.4. *In vitro* drug release

To investigate the release profiles. The required amount of DCX-loaded micelles (4 mL) were placed into dialysis tubes (SpectraPore®, MWCO 3500) introduced in 100 mL PBS buffer supplemented with 10% FBS at pH 7.4 and 2% (v/v) ethanol to enhance the solubility of released free DCX and avoid its aggregation.³⁴ The whole assembly was kept at 37 °C under stirring and covered by parafilm to avoid evaporation. At each sampling time 1 mL of medium were withdrawn and replaced with the same volume of fresh buffer (containing 2% (v/v) ethanol) to maintain the required sink conditions. Quantification was done by the calibration curve of DCX at 293 nm after dilution on methanol. Assays were carried out in triplicate.

Drug release profiles from the micellar systems were fitted to the square-root kinetics³⁵

$$M_t/M_\infty = k \cdot t^{0.5} \quad (5)$$

and to the Fickian diffusion model considering the micelles as perfect spheres³⁶

$$M_t/M_\infty = k_1 + k_2 \cdot t^{0.5} - k_3 \cdot t \quad (6)$$

where M_t and M_∞ represent the drug amount released at time t and that initially contained in the formulation, respectively, and k , k_1 , k_2 and k_3 are release rate coefficients, respectively.

2.5. Cellular uptake by fluorescence microscopy

Polymeric micelle uptake was followed by fluorescence microscopy by seeding HeLa cells on poly-L-lysine coated glass coverslips (12×12 mm²) placed inside 6-well plates (3 mL, 5·10⁴ cells/well) and grown for 24 h at standard culture conditions (5% CO₂ at 37 °C in Dulbecco's Modified Eagle Medium (DMEM) supplemented with 10% (v/v) FBS, 2 mM L-glutamine, 1% penicillin/streptomycin, 1 mM sodium pyruvate, and 0.1 mM MEM Non-Essential Amino Acids (NEAA)). Then, 50 µL of either DOXO loaded-polymeric micelle dispersions or free DOXO (0.005 µM DOXO) were added to cells. After 1 h and 24 h of incubation cells were washed three times with PBS pH 7.4 and, then, fixed with paraformaldehyde 4% (w/v) for 10 min, washed with PBS, permeabilized with 0.2% (w/v) Triton X-100). The cells were washed again with PBS, mounted on glass slides stained with ProLong® Gold antifade DAPI (Invitrogen) and cured for 24 h at -20 °C. Samples were visualized with 20X and 63X objectives using an inverted fluorescence microscope Leica DMI6000B (Leica Microsystems GmbH, Heidelberg Mannheim, Germany), whereby the blue channel corresponds to DAPI (λ_{ex} 355 nm), and the red channel to DOXO (λ_{ex} 475 nm).

2.6. *In vitro* copolymer cytocompatibility evaluation and cytotoxicity of drug-loaded polymeric micelles.

MDA-MB-231 adenocarcinoma breast and HeLa cervical cancer cells from Cell Biolabs (San Diego, CA, USA) were used for *in vitro* studies. Cells were grown at standard culture conditions (5% CO₂ at 37 °C) in Dulbecco's Modified Eagle Medium (DMEM) supplemented with 10% Fetal Bovine Serum (FBS), 2 mM L-glutamine, 1% penicillin/streptomycin, 1 mM sodium pyruvate, and 0.1 mM MEM Non-Essential Amino Acids (NEAA).

Breast MDA-MB-231 and cervical HeLa cancer cells with an optical confluence of 80–90% were seeded into 96-well plates (100 μL, 1.5·10⁴ cells/well) and grown for 24 h at standard culture conditions in 100 μL growth medium. After 24 h of incubation at 37 °C and 5% CO₂, free DCX and DOXO solutions, and bare, single and dual-loaded polymeric micelles at different cargo loadings were added to cultured cells for the cytocompatibility evaluation of bare copolymers and the cytotoxicity efficiency determination of the polymeric nanocarriers, respectively, and the cells subsequently incubated from 24 to 72 h. Cells exposed to copolymer-free culture medium were used as a negative control (100% viability) in both types of experiments. Cytotoxicity was evaluated at different time points using the CCK-8 proliferation assay. After incubation, 10 μL of CCK-8 reagent was added to each well, and after 2 h the absorption at 450 nm of cell samples was measured with an UV-vis microplate absorbance reader (BioRad model 689, USA). Cell viability was calculated as:

$$\% \text{ viability} = (\text{Abs}_{\text{sample}} / \text{Abs}_{\text{control}}) \times 100 \quad (7)$$

where Abs_{sample} is the absorbance at 450 nm for cell culture samples with either bare copolymer solutions or drug formulations (free drugs and drug-loaded micelles), and $Abs_{control}$ for PBS controls. Assays were carried out in triplicate.

3. Results and Discussion

Marketed intravenous formulation of chemotherapeutic drugs involve the use of organic solvents and/or surfactants to enhance their solubilization for injection in order to achieve the required therapeutic doses. This is the case, for example, of paclitaxel (PCX, Taxol[®]) and DCX (Taxotere[®]) which utilize Cremophor El and ethanol or polysorbate 80, respectively, for solubilization⁷ and avoidance of drug degradation in protic solvents³⁷. Specifically, DCX is a taxane compound that displays a broad spectrum of antitumor activity which interferes with microtubule formation during cell division,³⁸ and it is currently approved for the treatment of breast, non-small-cell lung, prostate, stomach, head and neck cancers.^{37,39} DCX is also used in combination with DOXO (supplied in saline formulation, Andryamicin[®]), an anthracycline antibiotic which intercalates into nuclear DNA and interacts with topoisomeraseII to cause DNA cleavage and cytotoxicity⁴⁰ in the treatment of advanced or metastatic breast cancer^{41,42} given their different mechanisms of action and partially non-overlapping toxicity profiles. However, there still exist severe side effects associated with the administration of these two drugs. Earlier studies have shown that the polysorbate 80 formulation of DCX cause severe allergic reactions and peripheral neuropathy in up to 40% of patients^{43,44}; after dilution with the hydroalcoholic vehicle provided, the Taxotere[®] formulation is physically unstable and must be administered to the patient within 8 h. On the other hand, DOXO binding to cell membranes ultimately results in the production of active oxygen species attacking

the myocytes, which is the main cause of severe DOXO cardiotoxicity.⁴⁵ Therefore, co-encapsulation on these two drugs in $\text{BO}_n\text{EO}_m\text{BO}_n$ polymeric micelles is expected to improve the efficiency and safety of the combinatorial treatment by acting on multiple pathways,⁴⁶ and even providing some kind of synergistic therapeutic effects while reducing acute toxicity and side effects^{20,21,47}.

Four $\text{BO}_n\text{EO}_m\text{BO}_n$ copolymers ($\text{BO}_8\text{EO}_{90}\text{BO}_8$, $\text{BO}_{14}\text{EO}_{378}\text{BO}_{14}$, $\text{BO}_{20}\text{EO}_{411}\text{BO}_{20}$ and $\text{BO}_{21}\text{EO}_{385}\text{BO}_{21}$) that cover a wide range of molecular weights and cmc values were chosen. These copolymers form spherical micelles ranging from 17 to 35 nm in diameter and association numbers between 20 and 43 (see Table1).^{48,49} At higher polymer concentrations viscous (from 1 to 6 wt.%) and immobile gels (> 5 wt.%, depending on copolymer type and solution temperature) appear as a consequence of the cross-linking originated from the residence of BO blocks in one polymer chain in two adjacent micelles promoting a progressively denser open network structure.

3.1.1 Cytocompatibility of $\text{BO}_n\text{EO}_m\text{BO}_n$ copolymers

To take into account potential differences in toxicity due to different cell phenotypes and sensitivity, we performed a comparative study to quantify how bare $\text{BO}_n\text{EO}_m\text{BO}_n$ polymeric micelles at different concentrations and incubation times (from 24 to 72 h) affect the *in vitro* viabilities of two tumoral cells lines of cervical (HeLa) and metastatic breast (MDA-MB-231) cancer by means of the cell-counting kit-8 cell proliferation assay (CCK-8). This test is based on the bioreduction of 2-(2-methoxy-4-nitrophenyl)-3-(4-nitrophenyl)-5-(2,4-disulfophenyl)-2H-tetrazolium monosodium salt (WST-8), which produces a water-soluble formazan dye in the presence of an electron carrier, 1-methoxy phenazinemethosulfate (PMS).

For HeLa cells, cell viabilities (CVs) between 90-100% were found for copolymer $\text{BO}_8\text{EO}_{90}\text{BO}_8$ in the whole concentration range. For the remaining copolymers, concentrations below 2 mg/mL led to viability extents above ca. 80% after 24 h and 72 h of incubation except for $\text{BO}_{21}\text{EO}_{385}\text{BO}_{21}$ with somewhat slightly lower values (Figure 1a). A certain cell viability loss was also noted as the copolymer concentration increases but always, in general, with CVs > 60%, larger than the limit of 50% considered as a reference value for a nanomaterial to be cytocompatible⁵⁰; there was an exception for copolymer $\text{BO}_{21}\text{EO}_{385}\text{BO}_{21}$ at the highest concentrations tested (4 mg/mL), for which CVs of ca. 40-42% denoted cell toxicity after 72 h of incubation (Figure 1a). Also, a certain decrease in CVs was found as the hydrophobic block length of the copolymers increases, especially noted for copolymer $\text{BO}_{21}\text{EO}_{385}\text{BO}_{21}$ which displayed the lower CVs. This behavior could stem from the greater affinity of the amphiphile for cellular membrane structures, increasing cell permeability.

Conversely, MDA-MB-231 cells were more sensitive to the presence of polymeric micelles exhibiting lower CVs, particularly after extensive incubation (72 h). A decrease in CV with incubation in MDA-MB-231 cells was also noted. For example, cells exposed to 4 mg/mL $\text{BO}_8\text{EO}_{90}\text{BO}_8$ micelles underwent a sharp viability loss from ca. 80% at 24 h of incubation to ca. 25% after 72 h. By contrast, under similar conditions the same copolymer showed viability extents of ca. 100% after 72 h of incubation in HeLa cells. $\text{BO}_{20}\text{EO}_{411}\text{BO}_{20}$ and $\text{BO}_{21}\text{EO}_{378}\text{BO}_{21}$ copolymers were toxic to MDA-MB-231 cells at the highest concentrations tested (> 3 mg/mL) after 72 h of incubation, the CVs being below 45 and 24% at 3 and 4 mg/mL, respectively (Figure 1b). At lower concentrations copolymer biocompatibility was observed, with CVs above 75 and 50% after 24 and 72 of incubation, respectively. Nevertheless, it is

here necessary to bear in mind that the cytotoxicity of $\text{BO}_n\text{EO}_m\text{BO}_n$ copolymers may be overestimated *in vitro* provided that cells are not protected by the anatomical barriers present *in vivo*.⁵¹ The present findings stressed the relevance of doing cytotoxicity tests in different cell lines in order to consider possible influences of cell phenotype on the cytocompatibility of a given material.

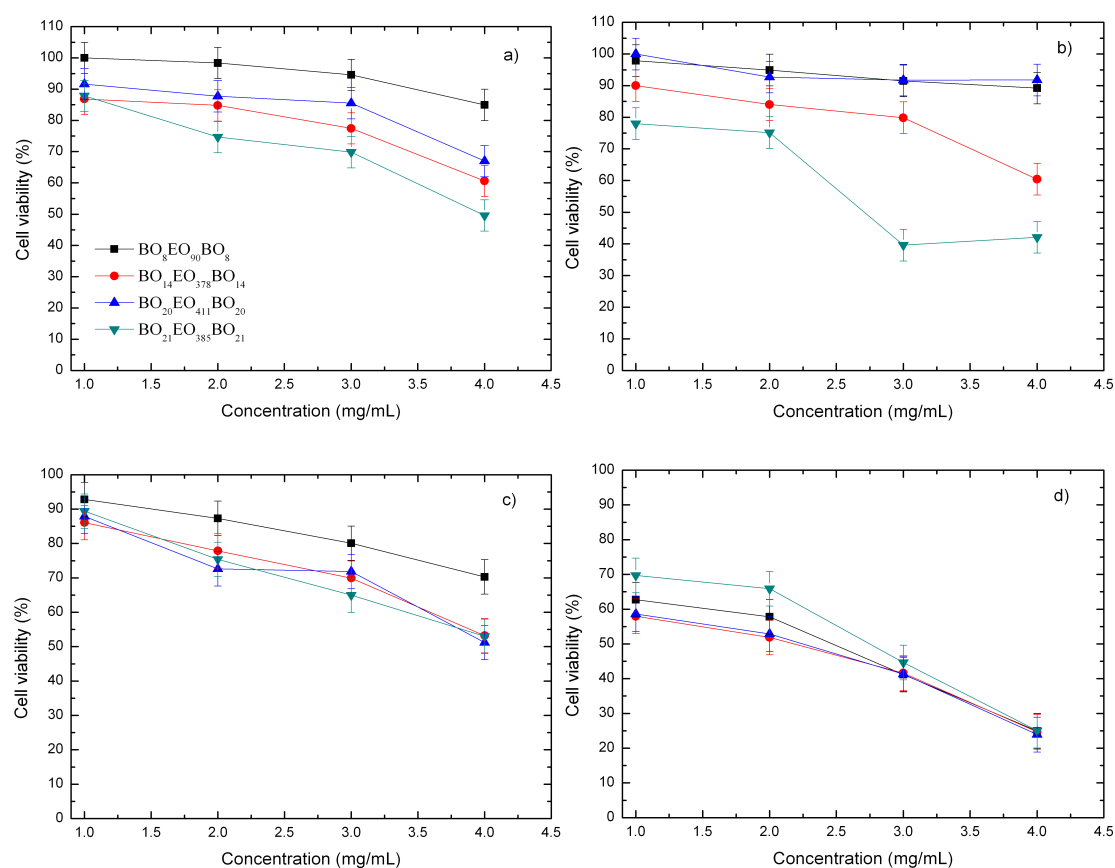


Figure 1: Cell viabilities of $\text{BO}_n\text{EO}_m\text{BO}_n$ polymeric micelles in HeLa cells after a) 24 and b) 72 h of incubation, and in MDA-MB-231 cells after c) 24 and d) 72 h of incubation.

3.1.2. Solubilization capacity

Different studies have reported that the major factor influencing the solubilization capacity of polymeric micelles is the compatibility between the drug

and the core-forming block.⁵²As commented previously, BO blocks are six times more hydrophobic than PPO units present in commercial Pluronic and Tetronic block copolymers (on the basis of their molar cmcs) so that a better compatibility between BO blocks and the present antineoplastic hydrophobic drugs might be expected in agreement with previous observation made with for much shorter diblock EO_mBO_n and triblock $\text{EO}_m\text{BO}_n\text{EO}_m$ copolymers.^{48,49}

Single (DCX) and dual (DCX/DOXO) encapsulation experiments were carried out to evaluate the impact of the feeding drug amount on the entrapment efficiency and the total loaded drug amount inside micelles by means of UV-Vis spectrophotometry and HPLC, when required. Preliminary attempts at dissolving DCX and DOXO into preformed micelles resulted in low drug loading probably because of the slow drug diffusion into the viscous micellar core (data not shown). Accordingly, it was decided to codissolve both the drug(s) and polymer in a pharmaceutically acceptable organic solvent (*i.e.* dichloromethane) to form a homogeneous polymeric matrix, followed by evaporation of the organic solvent and subsequent addition of the water phase. Hence, different amounts of drug(s) to solid copolymer (final polymer concentration usually 2 mg/mL, more than 10 times higher than the respective cmc ensuring complete micellization) were mixed to achieve different initial feeding ratios (see Table 2). For DCX-loaded and DOXO-loaded micelles²⁷ in the present solution conditions a maximum D.L. of ca. 0.9 and 1.1% (w/w) was obtained, respectively. The solubility of DCX and DOXO per gram of copolymer (S_{cp}) was concentration-dependent, reaching maximum values of up to ca. 9.2 and 10.2 mg g⁻¹, with solubility increments of ca. four and forty-fold the solubility of the pristine free drug(s) in water (5.5 and 0.5 mg/L, respectively).³² Among the different copolymers, $\text{BO}_{20}\text{EO}_{411}\text{BO}_{20}$ and $\text{BO}_{21}\text{EO}_{385}\text{BO}_{21}$ exhibited a slightly larger

solubilization capacity of DCX and DOXO which can be attributed to its longer hydrophobic blocks; at this respect, their extremely lengthy hydrophilic PEO blocks can also contribute to the copolymer to bear a more hydrophobic character. Conversely, $\text{BO}_8\text{EO}_{90}\text{BO}_8$ displayed the lower D.L. values possibly resulting from its smaller polymeric sizes which does not allow the solubilization of great amounts of drug. Focusing on DCX-loaded micelles developed in the present manuscript, as the drug/copolymer weight ratio increases the entrapment efficiency became lower as a consequence of the progressive DCX saturation of micelles (see Table 2) in agreement with previous observation for DOXO-loaded $\text{BO}_n\text{EO}_m\text{BO}_n$ micelles.²⁷ This leads to the assumption that micellar formulations could enhance the solubility of poorly soluble drugs but to a maximum limit after which any increase in the drug concentration can bring about drug precipitation. Nevertheless, full micellar saturation with DCX was not achieved in the light of D.L. data within the drug/copolymer ratios analyzed. In addition, the observed D.L. and E.E. for single DCX-loaded micelles were somewhat larger than those previously obtained for other block copolymers, for example, PEO–PPO-based block copolymers such as Pluronic^{®53} and Tetronic^{®54}, or PEO–poly[N-(2-hydroxypropyl)methacrylamide]-lactate copolymers,³⁶ but still lower than maximum values found for PEO-based block copolymers with other hydrophobic blocks such as poly(styrene oxide),³³ poly(lactic) acid,^{21,55} poly(caprolactone)⁵⁶ or poly(2-oxazoline)-based copolymers.⁵⁷

Table 2: Docetaxel loading, D.L., entrapment efficiency, E.E., and solubility per gram of copolymer, S_{CP} , of $\text{BO}_n\text{EO}_m\text{BO}_n$ copolymers.

Copolymers	DCX/copolymer (w/w %)	D.L. ^a (wt.%)	E.E. ^a (wt.%)	S_{CP}^b (mg/g)
$\text{BO}_8\text{EO}_{90}\text{BO}_8$	0.2	0.10	49.5	0.99
	0.5	0.24	46.1	2.31

	1.0	0.30	29.7	2.97
	2.0	0.40	20.0	4.01
	3.0	0.47	15.7	4.70
BO ₁₄ EO ₃₇₈ BO ₁₄	0.5	0.34	69.0	3.45
	1.0	0.49	49.5	4.95
	1.5	0.66	44.1	6.62
	2.0	0.70	35.5	7.10
	2.5	0.81	32.7	8.18
	3.0	0.89	30.0	9.00
	3.5	0.93	26.9	9.29
BO ₂₀ EO ₄₁₁ BO ₂₀	0.5	0.36	72.0	3.60
	1.0	0.49	49.5	4.95
	1.5	0.70	47.0	7.05
	2.0	0.77	38.8	7.75
	2.5	0.91	36.7	9.17
	3.0	1.01	34.2	10.25
	3.5	1.06	30.7	10.75
BO ₂₁ EO ₃₈₅ BO ₂₁	0.5	0.43	86.5	4.33
	1.0	0.48	48.5	4.85
	1.5	0.61	41.2	6.18
	2.0	0.68	34.4	6.87
	2.5	0.79	32.0	8.00
	3.0	0.87	29.2	8.75
	3.5	0.99	28.6	10.00

^a Estimated uncertainty $\pm 0.2\%$; ^b $\pm 1 \text{ mg g}^{-1}$

On the other hand, dual DCX/DOXO-loaded micelles were also prepared at different DCX/DOXO weight ratios while keeping the total drug and polymer concentrations constant during preparation. The drug solubilities are shown in Table 3. The presence of two drugs within BO_nEO_mBO_n micelles did not adversely affect the apparent solubility of the individual drugs; in fact, an increase in D.L. of copolymer micelles up to ca. 1.3% (w/w) was observed. Hence, it seems that the capacity of these BO_nEO_mBO_n micelles to incorporate drugs slightly increases when a co-loading process takes place, which points to a more suitable environment for drug solubilization inside the micellar cores possibly thanks to enhanced drug(s)-polymer interactions as previously observed, for example, for poly(2-oxazoline)-based

copolymers⁵⁷ and sterarate-grafter chitosan oligosaccharide micelles⁵⁸ to much larger extents. Also, the amount of the two drugs inside dual-loaded micelles was rather similar (when not a bit larger) as the single-loaded one sat similar initial loading concentrations of the single drug (data not shown). D.L. capacities in dual-loaded systems followed the same trend as in the case of single-loaded drugs, that is, the levels of drug encapsulation were higher for the most hydrophobic copolymers with the largest micellar cores, BO₂₀EO₄₁₁BO₂₀ and BO₂₁EO₃₈₅BO₂₁. Maximum D.L. values were also noted for most of the copolymer micelles at DCX/DOXO weight ratios of 50/50. In addition, E.E. of DCX was increased in the presence of DOXO inside the micellar core reaching values of ca. 94.5% for copolymer BO₂₀EO₄₁₁BO₂₀. The ability of the present micelles to load somewhat larger amounts of two anticancer drugs into the core is a behavior that needs further study but these findings are consistent with earlier investigations.^{21,59}

Table 3: Drug loading, D.L., entrapment efficiency, E.E., and solubility per gram of copolymer, S_{CP} , of the copolymers of dual (DCX/DOXO) loaded BO_nEO_mBO_n copolymer micelles.

Copolymers	DCX/DOXO (w/w %)	D.L. ^a (wt.%)	E.E. ^a (wt.%)	S_{CP}^b (mg/g)
BO ₈ EO ₉₀ BO ₈	75/25	0.31	45.1	3.16
	50/50	0.34	42.5	3.40
	25/75	0.32	35.6	3.20
	0/100	0.26	26.0	2.60
BO ₁₄ EO ₃₇₈ BO ₁₄	75/25	1.07	61.9	10.83
	50/50	1.16	58.8	11.75
	25/75	0.94	42.2	9.50
	0/100	0.79	32.0	8.00
BO ₂₀ EO ₄₁₁ BO ₂₀	75/25	1.06	61.2	10.71
	50/50	1.26	60.8	12.75
	25/75	1.22	54.7	12.32
	0/100	1.01	41.0	10.25
	75/25	0.93	53.5	9.37

BO ₂₁ EO ₃₈₅ BO ₂₁	50/50	1.06	53.8	10.75
	25/75	1.14	51.1	11.50
	0/100	1.03	41.5	10.38

3.1.3. Micellar size and stability of loaded polymeric micelles

Size distribution and dispersion stability of drug-loaded micelles are crucial factors for their successful parenteral application. Since particle size will not only affect endocytosis by tumor cells but also influences longevity during systemic circulation, micelles must be small enough to evade detection and destruction by the RES. Sizes and size distributions of DCX and DCX/DOXO loaded micelles were measured by DLS (for DOXO-loaded micelles see ref. 27). Micellar sizes ranged between 20 to 50 nm depending on the copolymer type with relatively monodisperse intensity distributions (Figure 2a). No important differences in sizes were observed between non-loaded, single and dual-loaded systems, and only a extremely slight size increased was observed as the loaded drug concentration was risen; however, a broader population size distribution could be observed for either single or dual-loaded micelles compared to non-loaded ones (Figure 2b). The absence of size increases in single and dual-loaded micelles could be attributed to the effect of hydrophobic interactions between aromatic rings of the drugs inside the micellar core and hydrogen bonds and van der Waals forces between hydroxy groups of drug(s) and block copolymers.⁶⁰ (Co)-loaded micelles could be readily freeze-dried and their initial size distribution was recovered upon reconstitution in aqueous solution, as observed previously²⁷ (data not shown).

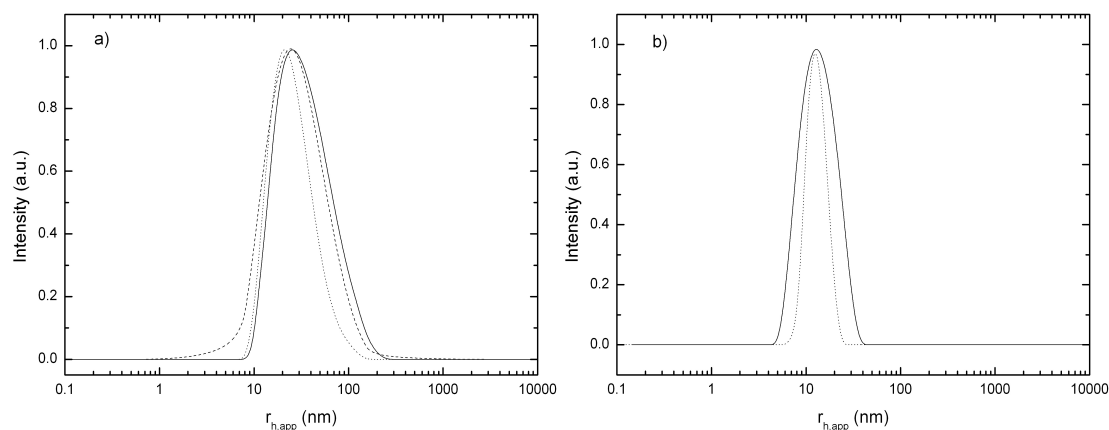
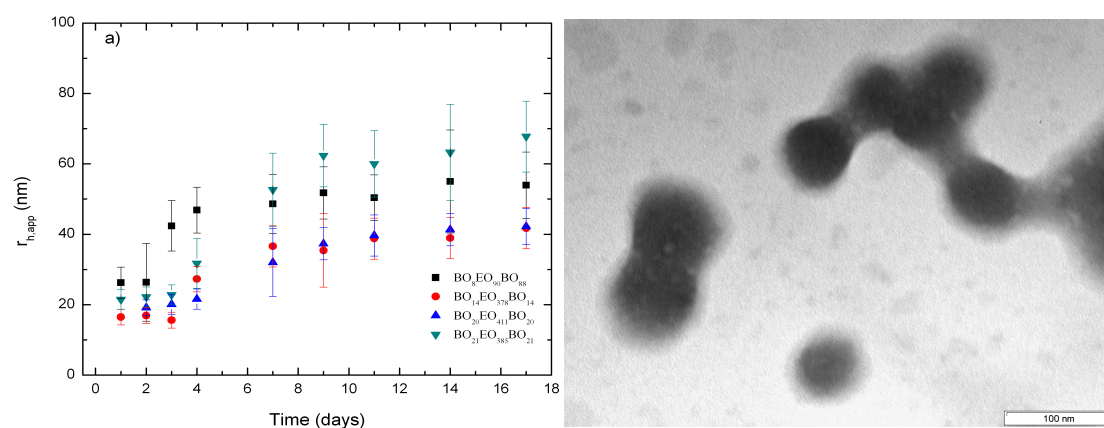


Figure 2: a) Intensity fraction size distributions of bare polymeric micelles of copolymers $\text{BO}_{14}\text{EO}_{378}\text{BO}_{14}$ (·····), $\text{BO}_{20}\text{EO}_{411}\text{BO}_{20}$ (- - -) and $\text{BO}_{21}\text{EO}_{385}\text{BO}_{21}$ (—) at 25 °C in PBS buffer pH 7.4, and b) of unloaded (·····) and DCX/DOXO-loaded $\text{BO}_8\text{EO}_{90}\text{BO}_8$ polymeric micelles under similar conditions.

Formulation challenges such as stability and drug–drug compatibility need to be considered in multiple drug delivery in a single dosage form. Hence, the stability over time of single DCX and dual-loaded DCX/DOXO polymeric micelles was tested in serum mimicking conditions by monitoring the micellar size evolution. In particular, for dual DCX/DOXO-loaded micelles sizes were observed to increase ca. 20 to 35 nm after 3-4 days of incubation depending on the copolymer type (Figure 3a), being the larger increase found for copolymer $\text{BO}_{21}\text{EO}_{385}\text{BO}_{21}$ (ca. 35 nm) and relatively similar for the three remaining ones (ca. 20-25 nm). Similar behavior was found for single DCX-loaded micelles (not shown). In the present case, a synergistic improvement of micelle stability in the present multidrug-loaded micelles is not achieved in contrast to what observed by Kwon *et al.*, for which an enhanced stability in dual-loaded polyethylene glycol-poly(D,L-lactide) (PEG-PDLA) copolymer micelles was noted as a consequence of possible favorable drug-drug interactions through H-bonding inside micelles.^{21,57} Moreover, our present data point to the fusion of adjacent loaded micelles into larger ones (see Figure 3b) in order to provide a more

suitable environment to the cargo and minimize serum protein binding. These changes can be a consequence of the reverse structure of the present copolymers: Upon micellization, copolymer chains must display two tight-junctions at the micellar core-corona interface which may lead to the preclusion of some hydrophobic blocks outside the micellar core configuring a less compact micellar interior and favoring the formation of intermicellar bridges;^{48,49} hence, to avoid drug contact with the biological external environment and subsequent protein binding, a structural rearrangement of micelles can take place. This picture is corroborated by TEM images, where the spherical micellar morphology can be observed to be still retained; however, drug loaded-micelles (either single or dual ones) upon extended incubation seem to be formed by a larger surrounded by a more loosely thicker corona than as-prepared loaded copolymer micelles (Figure 3c,d). Micellar sizes observed by TEM are also slightly smaller than those obtained by DLS but still comparable despite TEM analysis is performed under ambient (dry) conditions while DLS determines the hydrodynamic diameter (“equivalent sphere diameter”), *i.e.* the size of swollen and hydrated particle in an aqueous phase¹⁷. Whatever the case, after extensive incubation in the present conditions the single and dual loaded-polymeric micelles were still below ca. 100-120 nm in size, which enable their tumor-specific accumulation via the EPR effect.



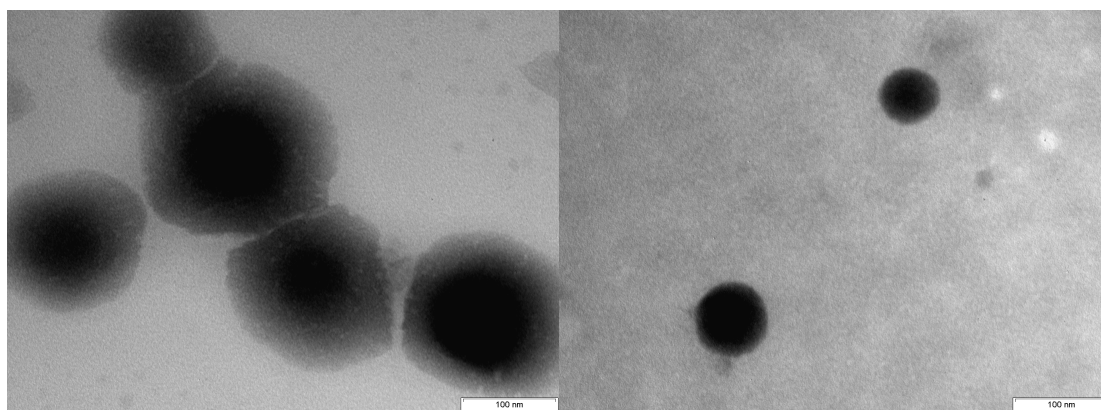


Figure 3: a) Temporal evolution of micellar sizes of dual-loaded $\text{BO}_n\text{EO}_m\text{BO}_n$ copolymers. TEM images of dual DCX/DOXO loaded $\text{BO}_{21}\text{EO}_{385}\text{BO}_{21}$ micelles b) during and c) after restructuration. d) TEM image of just-prepared dual DCX/DOXO loaded $\text{BO}_{21}\text{EO}_{385}\text{BO}_{21}$ micelles.

To ensure the delivery of the carried drug(s) to the site of action, the micellar carrier must be able to resist rapid dissociation upon dilution and exposure to blood plasma conditions. Hence, the physical stability of DCX-loaded and DCX/DOXO-loaded micelles was tested upon high dilution (1/50) in PBS buffer pH 7.4 containing 10% FBS at 37 °C to simulate *in vivo* parenteral administration by monitoring the free DCX concentration in solution over time (final copolymer concentrations were well below the cmc). DCX-loaded polymeric micelles remained stable upon extensive incubation, at least for 20 days, in the protein rich medium (Figure 4a). All the systems remained physically stable until day 3, the DCX solubility being above 90% of the initial value. As opposed to $\text{BO}_{20}\text{EO}_{411}\text{BO}_{20}$ and $\text{BO}_{21}\text{EO}_{378}\text{BO}_{21}$ micelles showing high stability over time (above 75% of the initial value after 20 days of incubation), $\text{BO}_8\text{EO}_{90}\text{BO}_8$ ones gradually lost DCX, 60% remaining at day 8 and ca. 35% after day 20. $\text{BO}_{14}\text{EO}_{378}\text{BO}_{14}$ micellar nanocarrier also showed a slight DCX concentration loss, with 85% remaining at day 8 and ca. 60% after 20 days (Figure 4a).

For dual-loaded micelles similar observations as for single-loaded micelles were noted (Figure 4b). By monitoring DCX release, it could be observed that all copolymers displayed stabilities larger than 85% after 3-4 days of incubation, and for $\text{BO}_{20}\text{EO}_{411}\text{BO}_{20}$ and $\text{BO}_{21}\text{EO}_{378}\text{BO}_{21}$ micelles being above 73% after 20 days. $\text{BO}_8\text{EO}_{90}\text{BO}_8$ micelles gradually lost DCX, 60% remaining at day 8 and ca. 32% after day 20, whilst $\text{BO}_{14}\text{EO}_{378}\text{BO}_{14}$ ones showed a better stability than the former, with 79% remaining at day 8 and ca. 56% after 20 days. Hence, the largest resistance to disintegration observed for $\text{BO}_{20}\text{EO}_{411}\text{BO}_{20}$ and $\text{BO}_{21}\text{EO}_{378}\text{BO}_{21}$ loaded micelles is in agreement with its larger hydrophobic chains that would favor a larger core providing a more suitable environment for the drug while decreasing interactions with water. The observed DCX retention values inside $\text{BO}_n\text{EO}_m\text{BO}_n$ micelles were larger than those observed for other structurally related polyethylene oxide (PEO)-based copolymers such as polyethylene oxide-propylene oxide (PEO-PPO)-based ones such as Pluronics and Tetronics,^{36,61} poly(N-vinylpyrrolidone)-poly(D,L-lactide) (PVP-PDLL)⁶² or PEG-PDLA ones,²¹ and rather similar to those observed for more hydrophobic copolymers such as polystyrene oxide-polyethylene oxide (PSO-PEO)⁶³ and polyethylene glycol-polycaprolactone ones (PEG-PCL),⁶⁴ or mixed polymeric micelles of polyethylene glycol-poly(D,L-lactic acid/D- α -tocopheryl polyethylene glycol 1000 succinate/stearic acid-modified chitosan polymers.⁶⁰

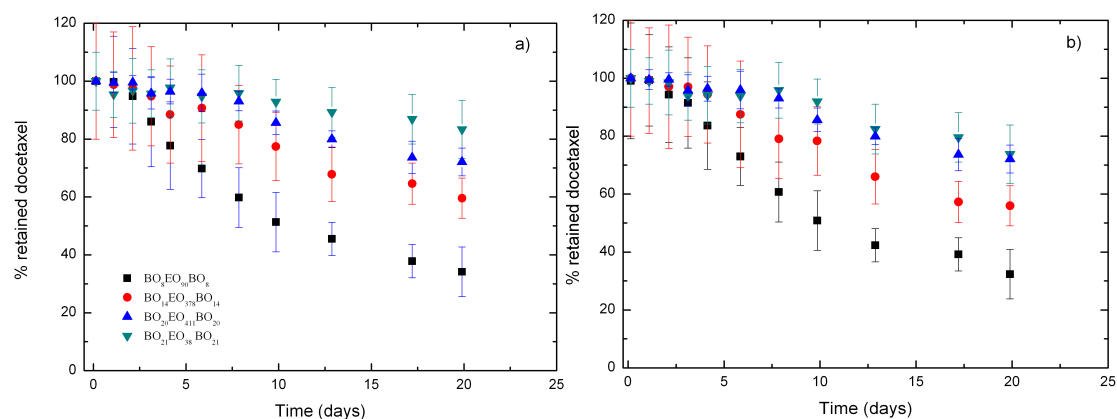


Figure 4: Temporal evolution of micelle stability in terms of DCX retained in a) single and b) dual-loaded $\text{BO}_n\text{EO}_m\text{BO}_n$ micelles over time at 37 °C in PBS buffer pH 7.4 supplemented with 10% FBS.

3.1.4 *In vitro* release kinetics

The release of DCX from polymeric micelles was assayed using dialysis tubing (Spectra Pore, cellulose ester membrane cutoff 3500 Da) that ensured that no micellar diffusion occurred. Release profiles for single and dual-drug loaded micelles in physiological mimicking medium (pH 7.4) are shown in Figure 5a,b. For single DCX-loaded micelles the release profiles were rather similar for all the copolymers, and characterized by the existence of an initial burst phase (Figure 5a) in which ca. 41, 38, 40, and 38% DCX along the first 5 h of incubation was released from $\text{BO}_8\text{EO}_{90}\text{BO}_8$, $\text{BO}_{14}\text{EO}_{378}\text{BO}_{14}$, $\text{BO}_{20}\text{EO}_{411}\text{BO}_{20}$ and $\text{BO}_{21}\text{EO}_{385}\text{BO}_{21}$ copolymers, respectively. The former phase was then followed by a sustained release pattern with ca. 92, 86, 81 and 79% DCX released after 30 h from each kind of polymeric micelle, respectively. The release profiles and the individual drug release rates practically did not change for dual-loaded micelles compared to the single-loaded ones. Dual micelles containing DCX and DOXO also showed the presence of an initial burst phase where ca. 39-45% and 34-42% of DCX and DOXO are released after 5 h of incubation, respectively, followed by the sustained pattern where 71 to 90% of DCX and 48 to 61% of DOXO are released after 30 h depending on the copolymer (Figure 5b).

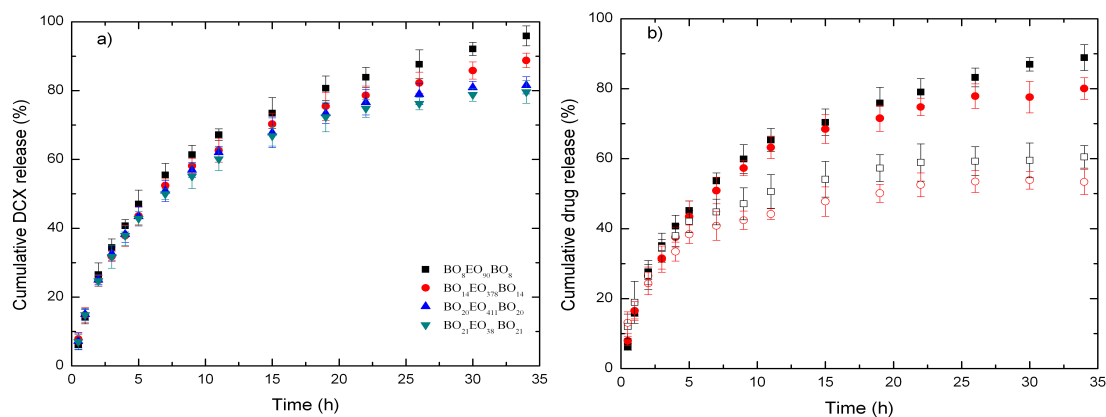


Figure 5: *In vitro* drug release of a) DCX and b) DCX (closed symbols) and DOXO (open symbols) from single and dual-loaded $\text{BO}_n\text{EO}_m\text{BO}_n$ polymeric micelles over time at 37 °C. Fit lines are not shown for clarity. In b) only release from $\text{BO}_8\text{EO}_{90}\text{BO}_8$ and $\text{BO}_{14}\text{EO}_{378}\text{BO}_{14}$ is shown for a better visualization.

The observed release profiles for both single and dual-loaded micelles might be the result of a certain disruption of the micellar system due to cohesion, higher concentration gradients, and/or sink conditions.⁵⁵ The amount of drug released from $\text{BO}_8\text{EO}_{90}\text{BO}_8$ micelles was larger than for the other polymeric micelles probably as a consequence of the slightly lower affinity between the drug and the shorter hydrophobic chains of this copolymer leading to smaller cores; conversely, a relatively higher retention of the drug inside the micellar structure was observed for the copolymers with longer BO blocks, $\text{BO}_{20}\text{EO}_{411}\text{BO}_{20}$ and $\text{BO}_{21}\text{EO}_{385}\text{BO}_{21}$.

The *in vitro* release profiles were fitted to the Higuchi³⁵ and Fickian diffusion models.³⁶ Tables 4 and 5 show that the latter model best fitted the experimental data on the basis of the correlation coefficient ($R^2 > 0.98$). This model takes into account drug diffusion, conformational changes in the micellar structure during release and partial transfer of drug from one micelle to another. At the beginning, with the uptake of water, micelles might swell and allow the drug within to diffuse through the pores.

However, the hydrophobic cores could retard the diffusion of water into the core, hence, decreasing the diffusion rate. The constant associated to drug diffusion (k_2) was rather similar (within uncertainty) for all copolymers investigated for both single and dual-loaded micelles, which points to a common mechanism of drug release independently of the type of cargo inside the polymeric micelles.

Table 4: Coefficients of DCX release from single-loaded $\text{BO}_n\text{EO}_m\text{BO}_n$ micelles.

Copolymer	Higuchi			Fickian				
	k	χ^2 reduced	R^2	k_1	k_2	k_3	χ^2 reduced	R^2
$\text{BO}_8\text{EO}_{90}\text{BO}_8$	17.74 (0.54)	44.93	0.951	- 15.60 (4.66)	32.32 (3.38)	2.32 (0.50)	16.00	0.983
$\text{BO}_{14}\text{EO}_{378}\text{BO}_{14}$	16.44 (0.46)	33.22	0.954	-8.16 (4.50)	25.953 (3.26)	1.62 (0.48)	14.92	0.980
$\text{BO}_{20}\text{EO}_{411}\text{BO}_{20}$	16.26 (0.71)	78.55	0.872	- 12.40 (3.44)	32.31(2.50)	2.81 (0.37)	8.73	0.986
$\text{BO}_{21}\text{EO}_{385}\text{BO}_{21}$	15.73(0.64)	62.29	0.900	- 14.30 (3.30)	31.81 (2.40)	2.72 (0.35)	8.05	0.987

Table 5: Coefficients of DCX and DOXO release from dual-loaded $\text{BO}_n\text{EO}_m\text{BO}_n$ micelles.

DOCETAXEL								
Copolymer	Higuchi			Fickian				
	k	χ^2 reduced	R^2	k_1	k_2	k_3	χ^2 reduced	R^2
$\text{BO}_8\text{EO}_{90}\text{BO}_8$	16.58 (0.54)	6.22	0.971	- 13.26 (0.94)	30.88 (0.95)	2.35 (0.16)	0.36	0.998
$\text{BO}_{14}\text{EO}_{378}\text{BO}_{14}$	16.00 (0.50)	4.54	0.958	- 11.26 (0.47)	29.42(0.41)	2.36 (0.07)	0.05	0.999

BO ₂₀ EO ₄₁₁ BO ₂₀	14.76 (0.51)	48.15	0.894	-9.41 (0.64)	27.60(0.45)	2.32 (0.06)	0.33	0.999
BO ₂₁ EO ₃₈₅ BO ₂₁	14.21(0.54)	55.41	0.869	- 11.61 (0.59)	28.84 (0.42)	2.60 (0.06)	0.28	0.998
DOXORUBICIN								
Copolymer	Higuchi			Fickian				
	k	χ^2 reduced	R ²	k ₁	k ₂	k ₃	χ^2 reduced	R ²
BO ₈ EO ₉₀ BO ₈	12.94 (0.68)	88.31	0.634	-1.52 (1.63)	23.37 (1.16)	2.23 (0.17)	2.17	0.991
BO ₁₄ EO ₃₇₈ BO ₁₄	11.55 (0.62)	73.59	0.594	-0.53 (1.65)	19.78 (1.17)	1.86 (0.17)	2.22	0.988
BO ₂₀ EO ₄₁₁ BO ₂₀	10.88 (0.64)	75.56	0.623	-0.67 (1.45)	17.34 (1.23)	1.65 (0.18)	2.33	0.987
BO ₂₁ EO ₃₈₅ BO ₂₁	10.34 (0.55)	67.89	0.644	-0.43 (1.22)	16.88 (1.11)	1.58 (0.15)	1.88	0.991

3.1.5. Internalization of drug-loaded micelles

To determine the potential use of this kind of polymeric micelles as potential drug delivery systems, *in vitro* cell internalization experiments were performed by exploiting the intrinsic fluorescence emission of DOXO chromophore observed by fluorescence microscopy. As observed in Figure 6a, after 1 h of incubation cell exposure to free DOXO caused a rapid drug accumulation inside cells, particularly in cell nuclei. In contrast, the fluorescence intensity was much lower after 24 h incubation as a result of certain cell death together with drug metabolization and subsequent excretion of the drug out of cells (Figure 6b).

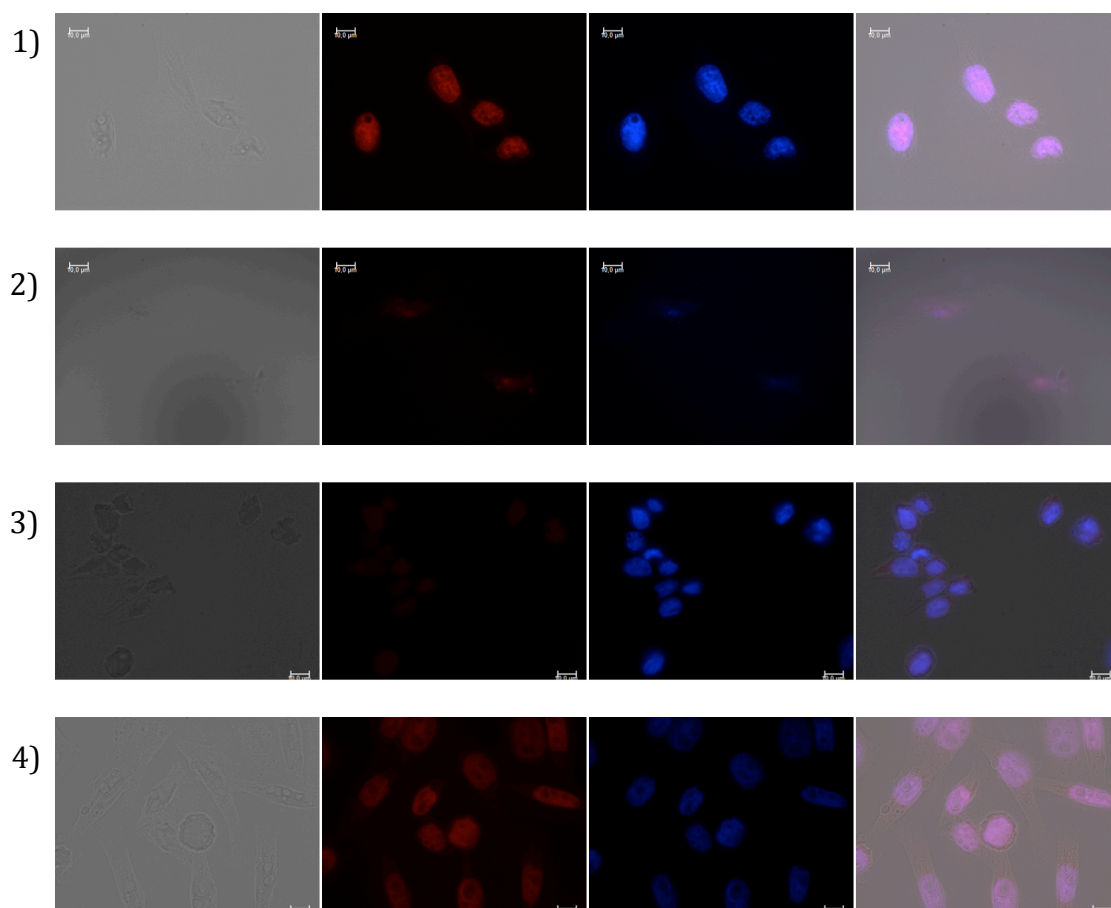


Figure 6: Fluorescence microscopy images of cellular uptake and intracellular distribution of drug-loaded $\text{BO}_n\text{EO}_m\text{BO}_n$ micelles. a) Bright field; b) DOXO-fluorescence (red-coloured, $\lambda_{\text{exc}} = 488 \text{ nm}$); c) blue fluorescence from cell nuclei stained with DAPI ($\lambda_{\text{exc}} = 355 \text{ nm}$); d) merged images of free DOXO after (1) 1 h and (2) 24 h of administration, and dual-loaded micelles after (3) 1 h and (4) 24 h of administration. Scale bar is $10 \mu\text{m}$.

Conversely, the distribution pattern changed significantly for drug administration inside single and dual drug-loaded micelles. Drug accumulation in cells was observed to increase with incubation time. The initial lower accumulation may be caused by the slower release of DOXO (and, also DCX) from micelles (see Figure 6c). The self-quenching effect of DOXO inside micelles makes fluorescence

observable only when DOXO is released.⁶⁵ After 24 h of incubation, DOXO fluorescence inside the cells was particularly intense, indicating that large drug amounts had been released from the micellar cores and are localized inside the cells (Figure 6d), mainly in nuclei but some still remaining in the cytoplasm. These findings support the hypothesis of a sustained drug release inside the cells. Preliminary experiments suggested that the cell uptake of drug-loaded $\text{BO}_n\text{EO}_m\text{BO}_n$ micelles would take place by an endocytosis-mediated mechanism, micelles being initially located within endosome vesicles enabling drug release in the cytosol in a sustained manner due to the endosome acidic environment.

3.1.6 Proliferation assay studies

The antiproliferative effects of single DCX and DOXO-loaded and dual DCX/DOXO-loaded $\text{BO}_n\text{EO}_m\text{BO}_n$ micelles at different polymer concentrations were evaluated by means of the CCK8 proliferation assay in breast MDA-MB-231 tumoral cell line, in which the sequential combinatorial administration of DCX and DOXO is used in advances or metastatic breast cancer. A MTT assay could not be used because DOXO interferes with the formation of formazan crystals.⁶⁶ In addition, the efficacy of treatments were further evaluated in cervical HeLa cancer cells in order to account for differences due to different cell phenotypes.

Single DCX and DOXO-loaded polymeric micelles exhibited a dose-dependent cytotoxic activity, *i.e.* the cell cytotoxicity increased as DOXO or DCX concentration released from the micelles does, in agreement with the observations for free drugs (Figure 7a,b). Also, they displayed a larger cell toxicity than free drugs at the same dose and incubation time and thus, larger IC_{50} values, as observed in Figure 7a,b. Provided that the copolymer showed to be cytocompatible at the concentration

used in the experiments (< 2 mg/mL for $\text{BO}_{14}\text{EO}_{378}\text{BO}_{14}$, $\text{BO}_{20}\text{EO}_{411}\text{BO}_{20}$ and $\text{BO}_{21}\text{EO}_{385}\text{BO}_{21}$, and < 5 mg/mL for $\text{BO}_8\text{EO}_{90}\text{BO}_8$), the enhancement in cell toxicity observed upon incubation with drug-loaded polymeric micelles can be ascribed to the cytotoxic effect of the loaded drug. This is compatible with an enhanced micelle accumulation inside the cell and a subsequent sustained drug release from the micelles, in agreement with fluorescence uptake data. This difference in toxicity can stem from the high stability of the micelles *in vitro* and the sustained drug release which results in more drug being available to exert its therapeutic effect for longer times on both cancer cell lines. In this regard, in spite of free drugs can rapidly enter inside cells they may be subsequently diffused out from cells, for example, through efflux pump mechanisms, decreasing their residence time.⁶⁷ Amongst the different single drug-loaded polymeric micelles those made of copolymer $\text{BO}_8\text{EO}_{90}\text{BO}_8$ displayed the largest cell toxicities, specially in the low to moderate drug concentration range (< 10 μM), probably as a consequence of their faster release from the micelle interior. For example, viabilities of only 13, 23, 28 and 32% were found for micelles of copolymers $\text{BO}_8\text{EO}_{90}\text{BO}_8$, $\text{BO}_{14}\text{EO}_{378}\text{BO}_{14}$, $\text{BO}_{20}\text{EO}_{411}\text{BO}_{20}$ and $\text{BO}_{21}\text{EO}_{385}\text{BO}_{21}$ at a DCX concentration of 9 μM in MDA-MB-231 cancer cells after 72 h of incubation, respectively (Figure 7a). At larger concentrations, cell toxicities became rather similar for all the copolymers since the amount of released drug is high enough to provide a huge cell death ($> 90\%$).

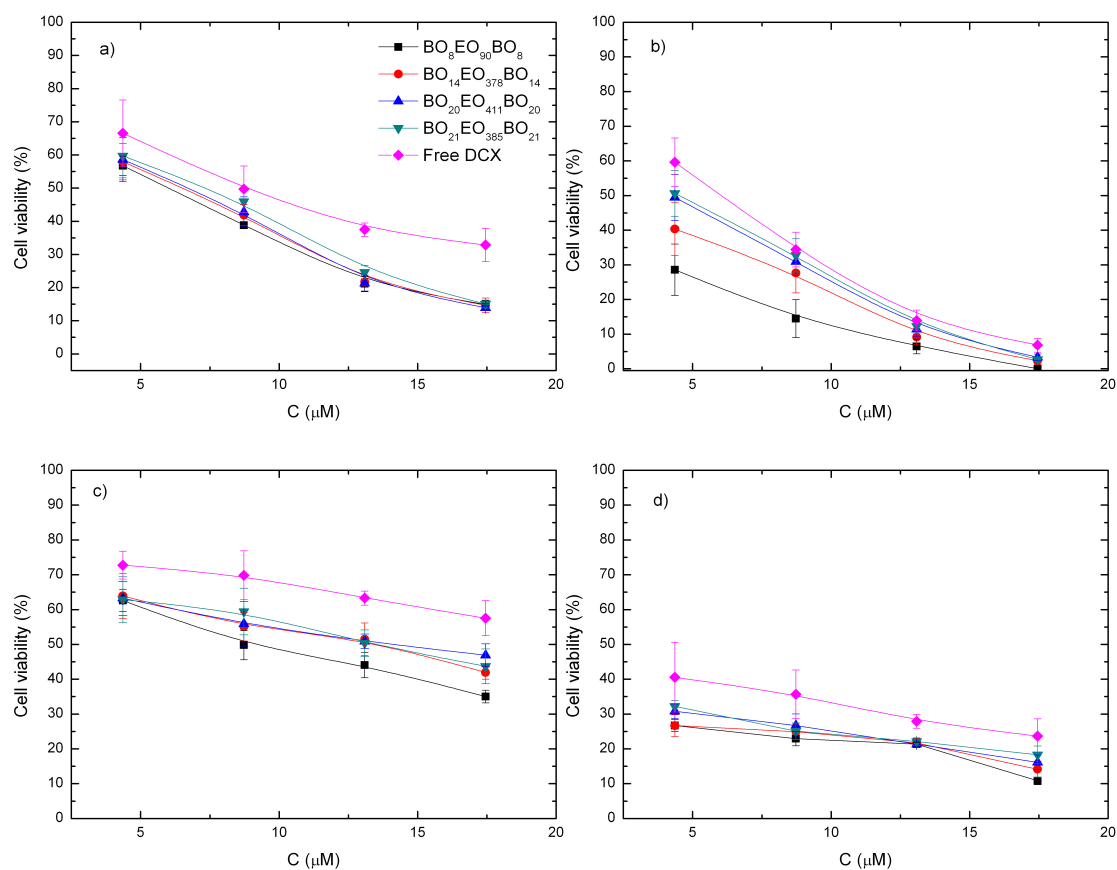


Figure 7: Cell viabilities of a) DCX and b) DOXO-loaded polymeric micelles in MDA-MB-231 breast cancer cells after 72 h of incubation, and of DCX-loaded polymeric micelles in HeLa cells after c) 24 and d) 72 h of incubation.

Cell proliferation was also observed to be enhanced with incubation time as a consequence of the progressive drug release (Figure 7c). For example, growth inhibition caused by polymeric micelles loaded with 17.5 μM DCX decreased from 35%, 42%, 47 and 44% at 24 h to 11%, 14%, 16% and 18% at 72 h of incubation for $\text{BO}_8\text{EO}_{90}\text{BO}_8$, $\text{BO}_{14}\text{EO}_{378}\text{BO}_{14}$, $\text{BO}_{20}\text{EO}_{411}\text{BO}_{20}$ and $\text{BO}_{21}\text{EO}_{385}\text{BO}_{21}$, respectively. Similar behavior was observed previously, for example, for DCX-loaded poly(ethylene oxide)-poly(styrene oxide)³³ and poly(*N*-vinylpyrrolidone)-poly(D,L-lactide) micelles upon cargo release.^{33,68} Moreover, despite both cell lines were largely affected by the presence of the antineoplastic drugs, HeLa cells were observed

to be slightly more sensitive (Figure 7d), specially to DOXO.

On the other hand, the cytotoxicity of DCX/DOXO loaded in the present polymeric micelles were evaluated at different drug weight ratios. DCX/DOXO weight ratios close to 50:50 were observed to be the most effective to inhibit cell proliferation (see Figure 8a as an example). To further analyze whether DCX and DOXO combinations are synergistic, additive, or antagonistic against HeLa and MDA-MB-231 proliferation, the combination indices for the various dosing ratios were calculated using Compusyn⁶⁹ software. The calculated CI values of some of the free drugs combinations in DMSO as well as most of dual drug-loaded micelles were well below 1.0 (Figure 8b), indicating a synergistic antiproliferative effect against both types of cancer cells, specially for MDA-MB-231 cancer cells at ratios close to 50:50 in weight. Similar findings were also reported, for example, upon dual administration of paclitaxel and rapamycin drug-loaded combinations in poly(ethylene glycol)-poly(lactide) (PEG-PLA) micelles to different tumor cell lines,⁵⁶ and dual-loaded etoposide/17-allylamino-17-demethoxygeldanamycin and bortezomib/17-allylamino-17-demethoxygeldanamycin poly(2-oxazoline) micelles.⁵⁴ Nevertheless, it is worth pointing out that further optimization of drug ratios is required, especially in *in vivo* models for which an understanding of the pharmacokinetics and pharmacodynamics of each individual drug in the multidrug composition is needed.

Cytotoxicity assays of dual DCX/DOXO-loaded polymeric micelles of copolymers BO₁₄EO₃₇₈BO₁₄ and BO₂₀EO₄₁₁BO₂₀ (50/50 weight ratio) were performed in both HeLa and MDA-MB-231 cells. We chose these copolymers since they provided intermediate release rates and high cell cytotoxicities while using a lower polymer concentration than BO₈EO₉₀BO₈ to form micelles. We observed that cell cytotoxicities after administration of dual-loaded micelles were larger than those

obtained with free DCX/DOXO combined drugs or single-drug loaded micelles at similar doses, as observed in Figure 8c,d as examples, especially for the breast cancer cell line. For example, dual drug-loaded micelles of copolymer $\text{BO}_{14}\text{EO}_{378}\text{BO}_{14}$ ($9\ \mu\text{M}$ total drug concentration) showed a cytotoxicity of ca. 44% in MDA-MB-231 cells in contrast to ca. 55 and 69% for single DOXO and DCX-loaded ones (Figure 8c). Similar results were also found for copolymer $\text{BO}_{20}\text{EO}_{411}\text{BO}_{20}$ (Figure 8d).

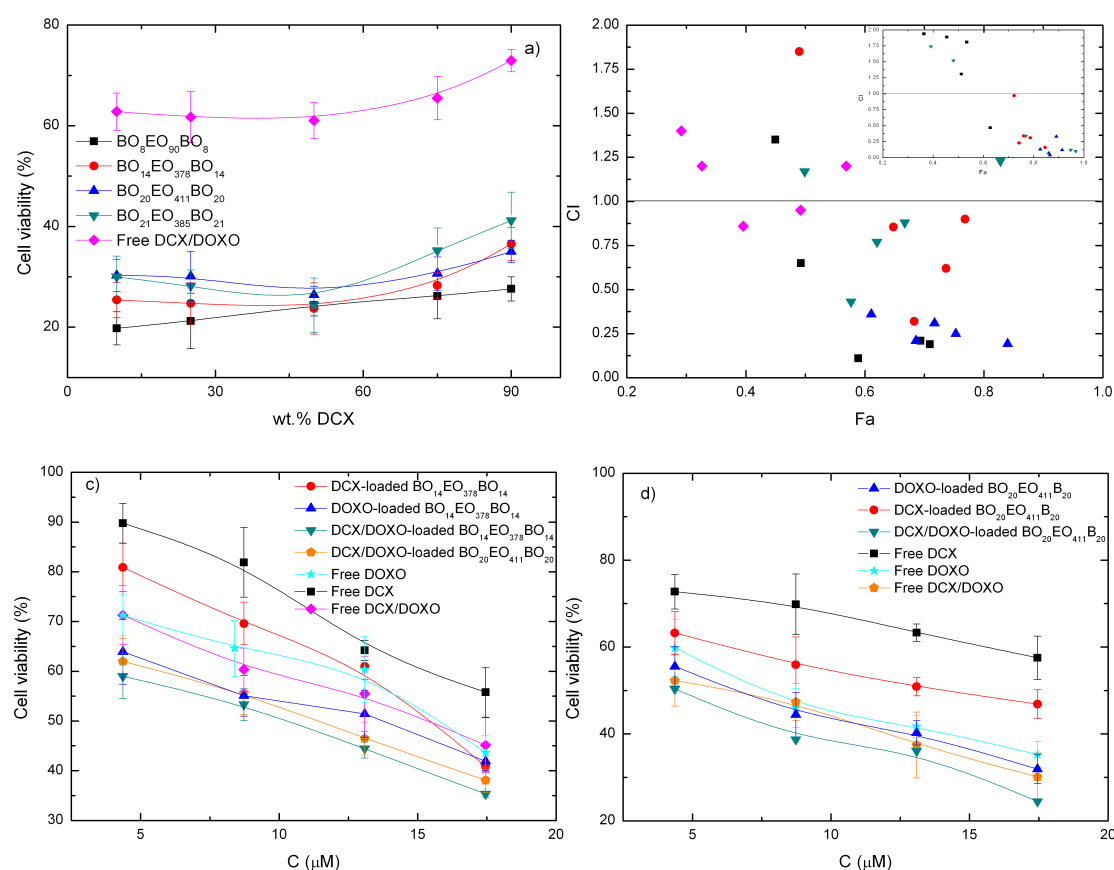


Figure 8: a) Cell viabilities and b) combination indices of free combined drugs and dual-loaded polymeric micelles at different weight ratios in MDA-MB-231 cancer cells after 24 h of incubation. Inset in b) denotes combination indices in HeLa cells. Cell viabilities of single free drugs, free combined drugs, single and dual-loaded micelles of c) copolymers $\text{BO}_{14}\text{EO}_{378}\text{BO}_{14}$ and $\text{BO}_{20}\text{EO}_{411}\text{BO}_{20}$ in MDA-MB-231 cells, and of d) copolymer $\text{BO}_{20}\text{EO}_{411}\text{BO}_{20}$ in HeLa ones after 24 h of incubation.

The observed larger proliferative inhibition effect of dual-loaded micelles again confirms the protection role and progressive release of drugs exerted by polymeric micelles and its subsequent intracellular accumulation leading to enhanced cell death. However, given that DCX and DOXO act by different mechanisms, combination therapy with these drugs within a single micelle can offer a new available therapeutic option to treat tumoral cells.

4. Conclusions

The existence of resistance to classical mono-chemotherapeutic cancer treatments and the clinical evidences of synergistic responses and reduced toxicity associated to higher doses of individual drugs in tumor treatments make combination therapy of chemotherapeutics a without standing approach to overcome the limitations of single-drug treatments. However, for the analyzed chemotherapeutics DOXO and DCX, currently used in the treatment of advanced and metastatic breast cancer, multiple drug combinations in a single delivery system are not yet commercially available. On the basis of these findings, we have selected $\text{BO}_n\text{EO}_m\text{BO}_n$ polymeric micelles as a vehicle for single and dual drug delivery of DCX and DOXO. We have shown that $\text{BO}_n\text{EO}_m\text{BO}_n$ micelles can effectively incorporated important amounts of both single and coloaded drugs. When coloaded, solubility extents are somewhat larger than in the case of single solubilized drugs. In addition, the present nanocarrier systems also provides a good stability, with a relatively slight micelle size increase after 3-4 days of incubation related to the fusion of adjacent micelles as a consequence of polymeric chain restructuration. The single and dual-loaded micelles can effectively deliver drugs to cancer cells. Both single- and dual-loaded micelles displayed larger cell toxicities than administered free drugs at the same doses. In

particular, DCX/DOXO-loaded micelles display synergistic effects against the two cancer cell lines (MDA-MB-231 and HeLa) tested. These synergistic effects were dependent on drug ratios, which require further optimization of the corresponding drug formulations. The combination of a slight increase in drug loading and the decrease in the amount of both the total drug and polymeric excipients to achieve similar cell cytotoxicities while eliminating the need of organic solvents/excipients for DCX/DOXO parenteral administration make the present $\text{BO}_n\text{EO}_m\text{BO}_n$ polymeric micelles appear an attractive drug delivery system and may have great advantage over current methods potentially increasing the safety of clinical interventions while minimizing adverse side effects. Moreover, the inhibition ability of the P-gp efflux pump of some of the present copolymer varieties would also provide a further complement to configure an “active” nanocarrier with a great potential therapeutic efficacy.

Acknowledgements

Authors thank Ministerio de Economía y Competitividad (MINECO) and Xunta de Galicia for research projects MAT 2013-40971-R and EM2013-046, respectively. Authors also specially thank staff of Instituto de Ortopedia y Banco de Tejidos Musculoesqueléticos of the Universidad de Santiago de Compostela, and specially to Maite Silva, for hepful assistance during *in vitro* cell experiments. S.B. greatly acknowledges MINECO for her Ramon y Cajal fellowship. E.V.A. is grateful to the Spanish Ministerio de Economía y Competitividad for FPU (AP2012-2921) fellowship.

REFERENCES

- (1) J. L. Arias, Drug targeting strategies in cancer treatment: an overview. *Mini-Rev. Med. Chem.* 2011, **11**, 1–17.
- (2) P. Y., Lee, K. K. Y. Wong, Nanomedicine: a new frontier in cancer therapeutics. *Curr. Drug Deliv.* 2011, **8**, 245–253.
- (3) J. Heidel, M. Davis, Clinical developments in nanotechnology for cancer therapy. *Pharm. Res.* 2011, **28**, 187–199.
- (4) M.C. Jones; J.C. Leroux. Polymeric micelles: a new generation of colloidal drug carriers. *Eur. J. Pharm. Biopharm.* 1999, **48**, 101–111.
- (5) V. P. Torchilin, Structure and design of polymeric surfactant- based drug delivery systems. *J. Control. Release* 2001, **73**, 137–172.
- (6) V. P. Torchilin, Micellar nanocarriers: pharmaceutical perspectives. *Pharm. Res.* 2007, **24**, 1–16.
- (7) G. Gaucher, M. H. Dufresne, V. P. Sant, N. Kang, D. Maysinger, J. C. Leroux, Block copolymer micelles: preparation, characterization and application in drug delivery. *J. Control. Release* 2005, **109**, 169–188.
- (8) D. G. Yu, G. R. Williams, X. Wang, X.-K. Liu, H.-L. Li, S. W. A. Bligh, Dual drug release nanocomposites prepared using a combination of electrospraying and electrospinning. *RSC Adv.* 2013, **3**, 4652-4658.
- (9) D.-G. Yu, F. Liu, L. cui, Z.-P. Liu, X. Wang, S. W. Bligh, Coaxial electrs spinning using a concentric Teflon spinneret to prepare biphasic-release nanofibers of helicid. *RSC Adv.* 2013, **3**, 17775-17783.
- (10) S. N. Ramaswamy, Rational design of cancer-drug combinations. *New Engl. J. Med.* 2007, **357**, 299-300.

- (11) H. Zhao, Z. Wei, S. Xu, M. Tang, L. Deng, J. Zhang, A. Dong, Preparation and properties of polymer micelle-embedded nanofibrous membranes for dual-drug co-delivery and multistep release. *RSC Adv.* 2015, doi:10.1039/C5RA03345D.
- (12) R. S., Finley, C. Balmer, Optimizing chemotherapy outcome. In R. S. Finley and C. Balmer (eds.). *Concepts in Oncology Therapeutics*, American Society of Health-System Pharmacists, Bethesda, MD, 1998, pp. 87-89
- (13) H. Gelderblom, J. Verweij, K. Nooter, A. Sparreboom, Cremophor EL: the drawbacks and advantages of vehicle selection for drug formulation. *Eur. J. Cancer* 2001, **37**, 1590-1598.
- (14) C. Alvarez-Lorenzo, A. Sosnik, A. Concheiro, PEO-PPO block copolymers for passive micellar targeting and overcoming multidrug resistance in cancer therapy. *Curr. Drug Targets* 2011, **12**, 1112–1130.
- (15) K. Mortensen, W. Batsberg, S. Hvidt, Effects of PEO-PPO diblock impurities on the cubic structure of aqueous PEO-PPO-PEO pluronic micelles: fcc and bcc ordered structures in F127. *Macromolecules* 2008, **41**, 1720–1727.
- (16) P. Taboada, G. Velasquez, S. Barbosa, Z. Yang, S. K. Nixon, Z. Zhou, F. Heatley, M. Ashford, V. Mosquera, D. Attwood, C. Booth, Micellization and drug solubilization in aqueous solutions of a diblock copolymer of ethylene oxide and phenyl glycidyl ether. *Langmuir* 2006, **22**, 7465–7470.
- (17) S. Barbosa, M. A. Cheema, P. Taboada, V. Mosquera, Effect of copolymer architecture on the micellization and gelation of aqueous solutions of copolymers of ethylene oxide and styrene oxide. *J. Phys. Chem. B.* 2007, **111**, 10920–10928.
- (18) M. Crothers, Z. Zhou, N. M. P. S. Ricardo, Z. Yang, P. Taboada, C. Chaibundit, D. Attwood, C. Booth, Solubilisation in aqueous micellar solutions of block copoly(oxyalkylene)s. *Int. J. Pharm.* 2005, **293**, 91–100.

- (19) M. E. N. P. Ribeiro, S. M. de Oliverira, N. M. P. S. Ricardo, S.-M. Mai, D. Attwood, S. G. Yeates, C. Booth, Diblock copolymers of ethylene oxide and 1,2-butylene oxide in aqueous solution: Formation of unimolecular micelles. *Int. J. Pharm.* 2008, **362**, 193–196.
- (20) H. C. Shin, A. W. Alani, H. Cho, Y. Bae, J. M. Kolesar, G. S. Kwon, A 3-in-1 polymeric micelle nanocontainer for poorly water soluble drugs. *Mol. Pharm.* 2011, **8**, 1257–1265.
- (21) H. C. Shin, A. W. Alani, D. A. Rao, N. C. Rockich, G. S. Kwon, Multi-drug loaded polymeric micelles for simultaneous delivery of poorly soluble anticancer drugs. *J. Control. Release* 2009, **140**, 294–300.
- (22) F. Heatley, G.-E. Yu, W. B. Sun, E. J. Pywell, R. H. Mobbs, C. Booth, Triad sequence assignment of the ^{13}C NMR spectra of copolymers of ethylene oxide and 1,2-butylene oxide. *Eur. Polym. J.* 1990, **26**, 583-592.
- (23) G.-E. Yu, Z. Yang, M. Ameri, C. Attwood, J. H. Collett, C. Price, C. Booth, Diblock copolymers of ethylene oxide and 1,2-butylene oxide in aqueous solution. Effect of E-block length distribution on self-association properties. *J. Phys. Chem. B.* 1997, **101**, 4394–4401.
- (24) A. Kellarakis, X.-F. Yuan, S.-M. Mai, Y.-W. Yang, C. Booth, Aqueous micellar solutions of a triblock copolymer of ethylene oxide and 1,2-butylene oxide, $\text{B}_{12}\text{E}_{114}\text{B}_{12}$. Scaling the viscoelasticity of fluid and gel. *Phys. Chem. Chem. Phys.* 2003, **5**, 2628-2634.
- (25) Z. Zhou, Y.-W. Yang, C. Booth, B. Chu, Association of a triblock ethylene oxide (E) and butylene oxide (B) copolymer ($\text{B}_{12}\text{E}_{260}\text{B}_{12}$) in aqueous solution. *Macromolecules* 1996, **29**, 8357-8361.

- (26) A. Cambón, J. Brea, M. I. Loza, C. Alvarez-Lorenzo, A. Concheiro, S. Barbosa, P. Taboada, V. Mosquera, Cytocompatibility and P-glycoprotein inhibition of block copolymers: Structure–activity relationship. *Mol. Pharm.* 2013, **10**, 3232-3241.
- (27) A. Cambón, A. Rey-Rico, D. Mistry, J. Brea, M. I. Loza, D. Attwood, S. Barbosa, C. Alvarez-Lorenzo, A. Concheiro, P. Taboada, V. Mosquera, Doxorubicin-loaded micelles of reverse poly(butylene oxide)-poly(ethylene oxide)-poly(butylene oxide) block copolymers as efficient "active" chemotherapeutic agents. *Int. J. Pharm.* 2013, **445**, 47-57.
- (28) M.E.N.P. Ribeiro, I. M. Cavalcante, N. M. P. S. Ricardo, S.-M. Mai, D. Attwood, S. G. Yeates, C. Booth, Solubilisation of griseofulvin in aqueous micellar solutions of diblock copolymers of ethylene oxide and 1,2-butylene oxide with lengthy B-blocks. *Int. J. Pharm.* 2009, **369**, 196-198.
- (29) D. Mistry, T. Annable, X.-F. Yuan, C. Booth, Rheological behavior of aqueous micellar solutions of a triblock copolymer of ethylene oxide and 1,2-butylene oxide: B₁₀E₄₁₀B₁₀. *Langmuir*. 2006, **22**, 2986-2992.
- (30) A. Cambón, M. Alatorre-Meda, J. Juárez, A. Topete, D. Mistry, D. Attwood, S. Barbosa, P. Taboada, V. Mosquera, Micellisation of triblock copolymers of ethylene oxide and 1,2-butylene oxide: Effect of B-block length. *J. Colloid Interface Sci.* 2011, **361**, 154-158.
- (31) J. Kim, J. E. Lee, S. H. Lee, J. H. Yu, J.H. Lee, T. G. Park, T. Hyeon, Designed fabrication of a multifunctional polymer nanomedical platform for simultaneous cancer-targeted imaging and magnetically guided drug delivery. *Adv. Mater.* 2008, **20**, 478-483.
- (32) S. H. Yalkowsky, Y. He, Handbook of aqueous solubility data. CRC Press, Boca Raton, FL ,2003.

- (33) M. Elsabahy, M. E. Perron, N. Bertrand, G.-E. Yu, J. C. Leroux, Solubilization of docetaxel in poly(ethylene oxide)-block-poly(butylene/styrene oxide) micelles. *Biomacromolecules*. 2007, **8**, 2250-2257.
- (34) K. K. Upadhyay, A. N. Bhatt, E. Castro, A. K. Mishra, K. Chuttani, B. S. Dwarakanath, C. Schatz, J. F. Le Meins, A. Misra, S. Lecommandoux, In vitro and in vivo evaluation of docetaxel loaded biodegradable polymersomes. *Macromol. Biosci.* 2010, **10**, 503-512.
- (35) H. Wang, J. Xu, J. Wang, T. Chen, Y. Wang, Y. W. Tan, H. Su, K. L. Chan, H. Chen, Probing the kinetics of short-distance drug release from nanocarriers tonanoacceptors. *Angew. Chem. Int. Ed.* 2010, **49**, 8426–8430.
- (36) Z. Wei, J. Hao, S. Yuan, Y. Li, W. Juan, X. Sha, X. Fang, Paclitaxel-loaded Pluronic P123/F127 mixed polymeric micelles: formulation, optimization and in vitro characterization. *Int. J. Pharm.* 2009, **376**, 176–185.
- (37) B. M. Rao, A. Chakraborty, M. K. Srinivasu, M. L. Devi, P. R. Kumar, K. B. Chandrasekhar, A. K. Srinivasan, A. S. Prasad, J. Ramanatham, A stability-indicating HPLC assay method for docetaxel. *J. Pharm. Biomed. Anal.* 2006, **41**, 676-681.
- (38) A. Sparreboom, O. van Tellingen, W. J. Nooijen, J. H. L. Beijnen, Preclinical pharmacokinetics of paclitaxel and docetaxel. *Anti-Cancer Drugs*. 1998, **9**, 1-17.
- (39) R. A. Walker, J. L. Jones, S. Chappell, T. Walsh, J. A. Shaw, Molecular pathology of breast cancer and its application to clinical management. *Cancer Metastasis Rev.* 1997, **16**, 5-27.
- (40) F. Zunino, G. Capranico, DNA topoisomerase II as the primary target of antitumoranthracyclines. *Anticancer Drug Des.* 1990, **5**, 307–317.
- (41) K. D. Miller, W. McCaskill-Stevens, J. Sisk, D. M. Loesch, F. Monaco, R. Seshadri, G. W. Sledge Jr., Combination versus sequential doxorubicin and docetaxel

as primary chemotherapy for breast cancer: A randomized pilot trial of the Hoosier Oncology Group. *J. Clin. Oncol.* 1999, **17**, 3033–3037.

(42) I. C. Smith, S. D. Heys, A. W. Hutcheon, I. D. Miller, S. Payne, E. J. Gilbert, A. K. Ah-See, O. Eremin, L. G. Walker, T. K. Sarkar, S. P. Eggleton, K. N. Ogston, Neoadjuvant chemotherapy in breast cancer: Significantly enhanced response with docetaxel. *J. Clin. Oncol.* 2002, **20**, 1456–1466.

(43) A. Ardavanis, D. Tryfonopoulos, I. Yiotis, G. Gerasimidis, N. Baziotis, G. Rigatos, Non-allergic nature of docetaxel-induced acute hypersensitivity reactions. *Anti-Cancer Drugs* 2004, **15**, 581-585.

(44) A. J. Tije, J. Verweij, W. J. Loos, A. Sparreboom, Pharmacological effects of fomulation vehicles: implications for cancer chemotherapy. *Clin. Pharmacokinet.* 2003, **42**, 665-685.

(45) J. M. Berthiaume, K. B. Wallace, Adriamycin-induced oxidative mitochondrial cardiotoxicity. *Cell Biol. Toxicol.* 2007, **23**, 15–25.

(46) Y. Bae, A. W. Alani, N. C. Rockich, T. S. Lai, G. S.; Kwon, Mixed pH-sensitive polymeric micelles for combination drug delivery. *Pharm. Res.* 2010, **27**, 2421–2432.

(47) J. R. Hasenstein, H.-C. Shin, K. Kasmerchak, D. Buehler, G. S. Kwon, K. R. Kozak, Antitumor activity of triolimus: a novel multidrug-loaded micelle containing paclitaxel, rapamycin, and 17-AAG. *Mol. Cancer Ther.* 2012, **11**, 2233–2242.

(48) A. Cambon, E. Figueroa-Ochoa, M. Blanco, S. Barbosa, J. F. A. Soltero, P. Taboada, V. Mosquera, Micellar self-assembly, bridging and gelling behaviour of two reverse triblock poly(butylene oxide)-poly(ethylene oxide)-poly(butylene oxide) copolymers with lengthy hydrophilic blocks. *RSC Adv.* 2014, **4**, 60484-60496.

(49) A. Cambon, E. B. Figueroa-Ochoa, J. Juárez, E. M. Villar-Alvarez, A. Pardo, S. Barbosa, J. F. A. Soltero, P. Taboada, V. Mosquera, Complex self-assembly of

reverse poly(butylene oxide)-poly(ethylene oxide)-poly(butylene oxide) triblock copolymers with long hydrophobic and extremely lengthy hydrophilic blocks. *J. Phys. Chem. B* 2014, **4**, 5258-5269.

(50) M. E. Cavet, K. L. Harrington, K. R. Vandermeid, K. W. Ward, J.-Z. Zhang, Comparison of the effect of multipurpose contact lens solutions on the viability of cultured corneal epithelial cells. *Cont. Lens Anterior Eye*. 2009, **32**, 171–175.

(51) J. S. Palmer, W. J. Cromie, R. C. Lee, Surfactant administration reduces testicular ischemia-reperfusion injury. *J. Urol.* 1998, **159**, 2136–2139.

(52) C. Allen, D. Maysinger, A. Eisenberg, Nano-engineering block copolymer aggregates for drug delivery. *Colloids Surf. B*. 1999, **16**, 3-27.

(53) Z. Liu, D. Liu, L. Wang, J. Zhang, N. Zhang, Docetaxel-loaded pluronic P123 polymeric micelles: in vitro and in vivo evaluation. *Int. J. Mol. Sci.* 2011, **12**, 1684-1696.

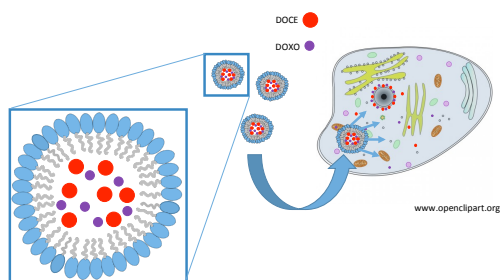
(54) C. Alvarez-Lorenzo, J. Gonzalez-Lopez, M. Fernandez-Tarrio, I. Sanchez-Macho, A. Cocheiro, Tetronic micellization, gelation and drug solubilization: Influence of pH and ionic strength. *Eur. J. Pharm. Biopharm.* 2007, **66**, 244-252.

(55) Y. Li, M. Jin, S. Shao, W. Huang, F. Yang, W. Chen, S. Zhang, G. Xia, Z. Gao, Small-sized polymeric micelles incorporating docetaxel suppress distant metastases in the clinically-relevant 4T1 mouse breast cancer model. *BMC Cancer* 2014, **14**, 329/1-329/15.

(56) A. S. Mikhail, C. Allen, Poly(ethylene glycol)-b-poly(ϵ -caprolactone) micelles containing chemically conjugated and physically entrapped docetaxel: Synthesis, characterization, and the influence of the drug on micelle morphology. *Biomacromolecules* 2010, **11**, 1273-1280.

- (57) Y. Han, Z. He, A. Schulz, T. K. Bronich, R. Jordan, R. Luxenhofer, A. V. Kabanov, Synergistic combinations of multiple chemotherapeutic agents in high capacity poly(2-oxazoline) micelles. *Mol. Pharm.* 2012, **9**, 2302-2313.
- (58) M. D. Zhao, F. Q. Hu, Y. Z. Du, H. Yuan, F. Y. Chen, Y. M. Lou, H. Yu, Coadministration of glycolipid-like micelles loading cytotoxic drug with different action site for efficient cancer chemotherapy. *Nanotechnology*. 2009, **20**, 055102.
- (59) G. P. Mishra, D. Nguyen, A. W. G. Alani, Inhibitory effect of paclitaxel and rapamycin individual and dual drug-loaded polymeric micelles in the angiogenic cascade. *Mol. Pharm.* 2013, **10**, 2071-2078.
- (60) J. Dou, H. Zhang, X. Liu, M. Zhang, G. Zhai, Preparation and evaluation in vitro and in vivo of docetaxel loaded mixed micelles for oral administration. *Colloids Surfaces B*. 2014, **114**, 20-27.
- (61) D. A. Chiappetta, C. Alvarez-Lorenzo, A. Rey-Rico, P. Taboada, A. Concheiro, A. Sosnik, N-alkylation of poloxamines modulates micellar assembly and encapsulation and release of the antiretroviral efavirenz. *Eur. J. Pharm. Biopharm.* 2010, **76**, 24–37.
- (62) D. Le Garrec, S. Gori, L. Luo, D. Lessard, D. C. Smith, M.-A. Yessine, M. Ranger, J. C. Leroux, Poly(N-vinylpyrrolidone)-block-poly(D,L-lactide) as a new polymeric solubilizer for hydrophobic anticancer drugs: in vitro and in vivo evaluation. *J. Control. Release*. 2004, **99**, 83-101.
- (63) A. Cambón, S. Barbosa, A. Rey-Rico, E. B. Figueroa-Ochoa, J. F. A. Soltero, S. G. Yeates, C. Alvarez-Lorenzo, A. Concheiro, P. Taboada, V. Mosquera, Poly(ethylene oxide)–poly(styrene oxide)–poly(ethylene oxide) copolymers: micellization, drug solubilization, and gelling features. *J. Colloid Interface Sci.* 2012, **387**, 275–284.

- (64) J. Jin, B. Sui, J. Gou, J. Liu, X. Tang, H. Xu, Y. Zhang, X. Jin, X. PSMA ligand conjugated PCL-PEG polymeric micelles targeted to prostate cancer cells. *Plos One*. 2014, **9**, e112200.
- (65) D. C. Rees, E. Johnson, O. Lewinson, ABC transporters: the power to change. *Nat. Rev. Mol. Cell Biol.* 2009, **10**, 218–227.
- (66) A. C. Collier, C. A. Pritsos, The mitochondrial uncoupler dicumarol disrupts the MTT assay. *Biochem. Pharmacol.* 2003, **66**, 281–287.
- (67) S. Kunjachan, B. Rychlik, G. Storm, F. Kiessling, T. Lammers, Multidrug resistance: physiological principles and nanomedical solutions. *Adv Drug Deliv. Rev.* 2013, **65**, 1852–1865.
- (68) V. Alakhov, E. Klinski, P. Lemieux, G. Pietrzynski, A. Kabanov, Block copolymeric biotransport carriers as versatile vehicles for drug delivery. *Expert Opin. Biol. Ther.* 2001, **1**, 583 – 602.
- (69) T.-C. Chou, N. Martin, CompuSyn software for drug combinations and for general dose- effect analysis, and user's guide. *ComboSyn, Inc. Paramus, NJ* 2007.
[www.combosyn.com]



TOC FIGURE

Reverse triblock copolymer micelles with lengthy polyethylene oxide blocks as efficient sustained dual drug-loaded nanocarriers